

The ‘Indian rope trick’ for a parametrically excited flexible rod: linearized analysis

BY ALAN R. CHAMPNEYS¹ AND W. BARRIE FRASER²

¹*Department of Engineering Mathematics, Queen’s Building,
University of Bristol, Bristol BS8 1TR, UK*

²*School of Mathematics and Statistics,
The University of Sydney, NSW 2006, Australia*

Received 19 May 1999; accepted 19 August 1999

It is well known that if a column exceeds a certain critical length it will, when placed upright, buckle under its own weight. In a recent experiment Mullin has demonstrated that a column that is longer than its critical length can be stabilized by subjecting its bottom support point to a vertical vibration of appropriate amplitude and frequency. This paper proposes a theory for this phenomenon.

Geometrically nonlinear dynamical equations are derived for a stiff rod (with linearly elastic constitutive laws) held vertically upwards via a clamped base point that is harmonically excited. Taking the torsion-free problem, the equations are linearized about the trivial response to produce a linear non-autonomous inhomogeneous partial differential equation (PDE). Solutions to this PDE are examined using two-timing asymptotics and numerical Floquet theory in an infinite-dimensional analogue of the analysis of the Mathieu equation. Good agreement is found between asymptotics and numerics for the conditions on amplitude and frequency of vibration for stabilizing an upside-down column that is longer than the critical length. A simple condition is derived for the lower bound on frequency for stability in terms of amplitude and the column’s length. An upper bound is more subtle, due to the presence of infinitely many resonance tongues inside the stability region of parameter space.

Keywords: rod mechanics; parametric excitation; inverted pendulum; Floquet theory; asymptotic analysis

1. Introduction

It has been known since the study by Stephenson (1908) that it is possible to stabilize a rigid pendulum in the ‘upside-down’ position by vibrating its pivot point vertically at high frequency. The recent book by Acheson (1997, ch. 12) describes a remarkable sequence of experiments performed by Tom Mullin. These experiments demonstrate that it is also possible to stabilize a coupled system of two or three jointed pendulums in this manner (Acheson & Mullin 1993), and even a piece of continuously flexible curtain wire which is beyond the critical length at which it would buckle under its own weight. In this paper we shall propose a theory for the latter experiment.

Acheson (1993) has proved a stability theorem for an upside-down configuration consisting of a system of n rigid simple pendulums smoothly jointed together to form a chain (see also Otterbein (1982) and Hurst (1996) for related results). The theorem

provides a simple condition on the amplitude and frequency of a vertical oscillatory excitation of the lowest pivot point in order for the chain of pendulums to be stabilized in the inverted position. The method is to use the theory of small oscillations based on Lagrange's equations of motion for the system. The normal modes of the system are shown to satisfy n uncoupled Mathieu equations. The condition on amplitude and frequency is then obtained by demanding that the eigenfrequencies of the chain all lie within the 'upside-down' stability boundary of the Mathieu equation.

The obvious next step is to let the length of the chain be fixed as the number of pendulums goes to infinity ($n \rightarrow \infty$). In this limit the Lagrange equation for a typical pendulum in the chain can be shown to pass to the equation of motion for a mass element of a continuous, perfectly flexible string a distance s along the string from the oscillating support pivot. Unfortunately, in this limit, the range of excitatory parameters which stabilize the inverted chain vanishes (the required frequency becomes infinite and the maximum allowed amplitude tends to zero), and this model fails to explain the 'Indian rope trick' under consideration here.

The question now arises as to the effect of a small amount of bending stiffness in the rope. This can be modelled by the introduction of a weak elastic restoring force at the joints that is proportional to the relative angle between the two adjacent pendulum rods. Although this model reduces to the equation for a beam in the continuum limit, the n Lagrange equations for the n -pendulum chain can no longer be transformed into n uncoupled Mathieu equations, and the previous method fails.

In this paper we deal directly with the continuum model. Section 2 presents a model which is a simplification of a more general dynamical model based on linear constitutive laws applied in a Frenet coordinate frame, allowing for more general forms of excitation. Section 3 considers applications of this model to the problem in question. It is argued that torsional deformation plays no role and that the effect of rotary inertia can be neglected. The equations are then linearized about the trivial state and the stability of this solution for the unforced problem is considered. Section 4 goes on to analyse the stability for the forced problem using regular asymptotic analysis. Section 5 then presents a numerical linear stability analysis, using Floquet theory to construct neutral stability curves. A comparison is made with the asymptotic results. Finally, §6 draws conclusions and suggests avenues for future research.

2. Mathematical formulation

Consider an initially straight column with a uniform circular cross-section of radius a , length ℓ and mass density m per unit length. The column is made of isotropic linearly elastic material so that the bending and torsional stiffnesses B and K are given by

$$B = \frac{1}{4}E\pi a^4, \quad K = \frac{1}{2}G\pi a^4, \quad (2.1)$$

where E is Young's modulus, $G = E/[2(1+\nu)]$ is the shear modulus and ν is Poisson's ratio. Thus B and K have the same order of magnitude.

A detailed derivation of the equations for the rate of change of linear and angular momentum for a moving rod relative to a rotating reference frame has been given recently by Fraser & Stump (1998). (Antman (1995) gives a more general Cosserat formulation, but since we take a circular cross-section and linear constitutive laws, we shall adopt here a simpler fixed-coordinate-system formulation.) To obtain the

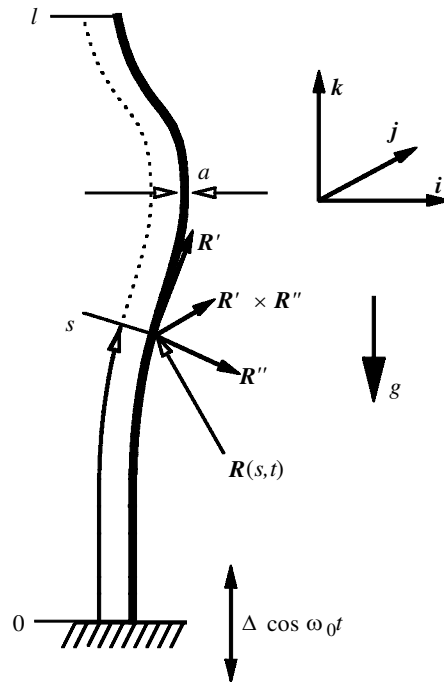


Figure 1. Definition sketch.

equations relative to an inertial reference frame $Oxyz$, with basis vectors $(\mathbf{i}, \mathbf{j}, \mathbf{k})$ with \mathbf{k} directed vertically up, set $\omega = \mathcal{V} = 0$ in eqns (2.3)–(2.11) of that paper. The rate of change of the linear momentum equation (2.3) becomes

$$mD^2\mathbf{R} = (T\mathbf{R}')' + \mathbf{V}' - mg\mathbf{k}, \quad (2.2)$$

where $\mathbf{R}(s, t)$ is the position vector, at time t , of a material point on the column axis that is a distance s from the bottom of the column (see figure 1). $T(s, t)$ is the tension, \mathbf{V} is the transverse shear force at the material point P, and g is the gravitational acceleration. $D = \partial/\partial t$ and $(\)' = \partial(\)/\partial s$. The rod is also assumed to have an inextensible axis so that $\mathbf{R}' \cdot \mathbf{R}' = 1$ and \mathbf{R}' is the unit tangent vector to the axis.

The angular velocity of a cylindrical element of the column at P is

$$\boldsymbol{\omega} = \omega_t \mathbf{R}' + \mathbf{R}' \times D\mathbf{R}', \quad (2.3)$$

where $\omega_t \mathbf{R}'$ is the component of the angular velocity of the cylindrical element at P about the column axis, and $\mathbf{R}' \times D\mathbf{R}'$ is the component about a diameter of the cross-section at P. Because the column is initially straight and its cross-section is circular, the angular momentum equation can be referred to unit basis vectors \mathbf{R}' , $\mathbf{n} = \mathbf{R}''/|\mathbf{R}''|$ and $\mathbf{b} = \mathbf{R}' \times \mathbf{n}$, which are, respectively, the tangent, principal normal and binormal vectors of the column axis. This leads to considerable simplification of the rod equations. For example, if the rod has a rectangular (not square) cross-section, the equations must be written with respect to unit basis vectors fixed in the material which do not usually coincide with $(\mathbf{R}', \mathbf{n}, \mathbf{b})$. In the present case the rate

of change of the angular momentum equation is (after substitution of results (2.3) into Fraser & Stump (1998), eqn (2.11))

$$\frac{1}{4}ma^2\{2D(\omega_t\mathbf{R}') + \mathbf{R}' \times D^2\mathbf{R}'\} = (Q\mathbf{R}')' + \mathbf{M}' + \mathbf{R}' \times \mathbf{V}. \quad (2.4)$$

To complete the formulation of the problem the following constitutive and constraint equations are required:

$$\left. \begin{aligned} \mathbf{M} &= B(\mathbf{R}' \times \mathbf{R}''), & Q &= KN' = K(\phi' - \mathbf{b}' \cdot \mathbf{n}), \\ \frac{\partial N}{\partial t} &= \omega_t, & \mathbf{R}' \cdot \mathbf{R}' &= 1, & \mathbf{V} \cdot \mathbf{R}' &= 0, \end{aligned} \right\} \quad (2.5)$$

where $N(s, t)$ is the rotation of the column cross-section at P relative to the section at the end $s = 0$. The torsion N' is the sum of two terms: (1) ϕ' where ϕ is the angle between the osculating plane of the column axis and a radial line (of material particles) joining the axis to a straight generator marked on the surface of an initially straight column; plus (2) the *tortuosity* ($\mathbf{b}' \cdot \mathbf{n}$) of the deformed column axis (Love 1927, ch. 18; Fraser & Stump 1998, eqns (2.15) and (2.18)).

Finally, let us see how torsional oscillations of the column can be treated independently of the deformation of the column axis and that they may therefore be dropped from further consideration in this problem. First, form the scalar product of \mathbf{R}' with equation (2.4) to obtain

$$\frac{1}{2}ma^2D\omega_t = Q'. \quad (2.6)$$

From equations (2.5)₂ and (2.5)₃ it can be seen that $D\omega_t' = D^2N' = (D^2Q)/K$, and when this result is introduced into the equation obtained from differentiating equation (2.6) with respect to s , the final result is

$$\frac{1}{2}ma^2D^2Q = KQ''. \quad (2.7)$$

This is the wave equation that governs the torsional oscillations of the column, and although free torsional oscillations of the column could be excited, since $Q = 0$ at the free top end of the column at $s = \ell$, it will be assumed that no initial condition is given to excite such oscillations. Hence torsion plays no role in the stability problem addressed here, and so $Q \equiv 0$ and $\omega_t \equiv 0$ is assumed from now on.

3. Application to the title problem

(a) Dimensionless model

In order to apply these equations to the present problem, where the bottom of the column is subject to a small oscillation in the vertical direction, set

$$\mathbf{R}(s, t) = \ell[\varepsilon \cos \omega_0 t \mathbf{k} + \mathbf{r}], \quad (3.1)$$

where ε is a dimensionless amplitude parameter, \mathbf{r} is the dimensionless position vector of P relative to the oscillating support point and ω_0 is the angular frequency of the excitation. Note that s is measured from the bottom of the column and not the inertial origin O. Other dimensionless variables appropriate to this problem are defined as follows:

$$\left. \begin{aligned} \bar{s} &= s/\ell, & \bar{\mathbf{R}} &= \mathbf{R}/\ell, & \bar{t} &= \omega_0 t, \\ \bar{T} &= \frac{T}{mg\ell}, & \bar{\mathbf{V}} &= \frac{\mathbf{V}}{mg\ell}, & \bar{B} &= \frac{B}{mg\ell^3}, & \delta &= \frac{g}{\omega_0^2\ell}, & \bar{D} &= \frac{D}{\omega_0}. \end{aligned} \right\} \quad (3.2)$$

When (3.1) is substituted into equations (2.2), (2.4) and (2.5), along with the dimensionless variables defined in (3.2), the results are

$$\bar{D}^2 \mathbf{r} - \mathbf{k} \varepsilon \cos \bar{t} = \delta[(\bar{T} \mathbf{r}')' + \bar{\mathbf{V}}' - \mathbf{k}], \quad (3.3)$$

$$\frac{1}{4}(a/\ell)^2 \mathbf{r}' \times \bar{D}^2 \mathbf{r}' = \delta(\bar{\mathbf{M}}' + \mathbf{r}' \times \bar{\mathbf{V}}), \quad (3.4)$$

$$\bar{\mathbf{M}} = \bar{B}(\mathbf{r}' \times \mathbf{r}''), \quad \mathbf{r}' \cdot \mathbf{r}' = 1, \quad \mathbf{r}' \cdot \bar{\mathbf{V}} = 0, \quad (3.5)$$

where $(\)' = \partial(\)/\partial \bar{s}$.

Since the aspect ratio of the column considered here is very small, $(a/\ell) \ll 1$, the rotary inertia term on the left-hand side of equation (3.4) will be neglected. When the constitutive relation (3.5)₁ is substituted into equation (3.4) with the left-hand side set to zero, and the cross-product of the resulting equation with \mathbf{r}' is formed, the result is

$$\bar{\mathbf{V}} = \delta B[\mathbf{r}' \times (\mathbf{r}' \times \mathbf{r}''')]. \quad (3.6)$$

The shear force $\bar{\mathbf{V}}$ can now be eliminated between equations (3.3) and (3.6) to give a final equation for the position vector $\mathbf{r}(s, t)$ and the tension \bar{T} , and this equation together with the inextensibility condition (3.5)₂ and suitable boundary and initial conditions constitutes a well-posed boundary-value problem.

Note. The overbars on the dimensionless quantities will be dropped as all variables are dimensionless from now on unless stated otherwise.

(b) Initial and boundary conditions

Initially the position $\mathbf{r}(s, 0)$ and velocity $D\mathbf{r}(s, 0)$ must be specified.

At the lower boundary, $s = 0$, it will be assumed that the column is built into the vibrating support system, and at the top end, $s = 1$, the column is completely free. Thus,

$$\left. \begin{aligned} \mathbf{r} &= \mathbf{0}, \quad \mathbf{r}' = \mathbf{k} \quad \text{at } s = 0, \\ \mathbf{M} = \mathbf{V} &= \mathbf{0} \quad \text{and} \quad T = 0, \quad \text{at } s = 1. \end{aligned} \right\} \quad (3.7)$$

(c) The vertically straight solution

The underlying solution whose stability is the subject of this paper is given by

$$\mathbf{r} = \mathbf{k}s. \quad (3.8)$$

When this form of \mathbf{r} is substituted into the above equations it is found that

$$\mathbf{M} = \mathbf{V} = \mathbf{0},$$

and equation (3.3) reduces to

$$\delta T' \mathbf{k} = (\delta - \varepsilon \cos t) \mathbf{k}.$$

This equation can be integrated with respect to s to give, after account is taken of the boundary conditions (3.7),

$$\delta T = -(\delta - \varepsilon \cos t)(1 - s). \quad (3.9)$$

(d) *Stability analysis of this solution*

Consider a perturbation to the above solution in the form of a small additional lateral displacement $\hat{\mathbf{r}}(s, t)$ so that

$$\mathbf{r} = \mathbf{k}s + \hat{\mathbf{r}} \quad \text{and} \quad \delta T = -(\delta - \varepsilon \cos t)(1 - s) + \delta \hat{T},$$

where $|\hat{\mathbf{r}}| \ll 1$ and $|\hat{T}| \ll 1$. This form is now substituted into equations (3.3)–(3.6) and only terms linear in the small quantities are retained. The inextensibility condition gives $\mathbf{k} \cdot \hat{\mathbf{r}} = 0$ and equation (3.6) gives $\mathbf{V} = \delta B(\mathbf{k} \times [\mathbf{k} \times (\hat{\mathbf{r}}''')]) = -\delta B\hat{\mathbf{r}}'''$. This last result and the expression for T are now substituted into equation (3.3) to obtain

$$D^2\hat{\mathbf{r}} = (\delta - \varepsilon \cos t)[\hat{\mathbf{r}}' - (1 - s)\hat{\mathbf{r}}''] - \delta B\hat{\mathbf{r}}'''' + \delta \mathbf{k}\hat{T}'.$$

Since $\hat{\mathbf{r}}$ and its derivatives are all perpendicular to \mathbf{k} , $\hat{T}' = 0$, which on integration and application of the boundary condition (3.7)₄ gives $\hat{T} = 0$. Finally, the equation governing the stability of solution (3.8) and (3.9) is

$$D^2\hat{\mathbf{r}} = -(\delta - \varepsilon \cos t)[(1 - s)\hat{\mathbf{r}}']' - \delta B\hat{\mathbf{r}}'''' , \quad (3.10)$$

and the boundary conditions (3.7) become

$$\begin{aligned} \hat{\mathbf{r}} &= \hat{\mathbf{r}}' = \mathbf{0}, & \text{at } s = 0, \\ \hat{\mathbf{r}}'' &= \hat{\mathbf{r}}''' = \mathbf{0}, & \text{at } s = 1. \end{aligned}$$

Equation (3.10) can be written in terms of its \mathbf{i} and \mathbf{j} components. Note that equations in each component will be identical. Appealing to the theory of symmetry-breaking bifurcations, physical instability modes will either be lateral or rotational. Without loss of generality, in the former case one may write $\hat{\mathbf{r}} = \mathbf{i}u(s, t)$ and in the latter $\hat{\mathbf{r}} = \mathbf{i}u(s, t) + \mathbf{j}v(s, t)$. Therefore, in either case, at the linear level the conditions for the stability of the vertically upright solution become

$$D^2u = -(\delta - \varepsilon \cos t)[(1 - s)u']' - \delta Bu'''' , \quad (3.11)$$

and

$$\left. \begin{aligned} u &= u' = 0, & \text{at } s = 0, \\ u'' &= u''' = 0, & \text{at } s = 1. \end{aligned} \right\} \quad (3.12)$$

(e) *The unforced problem: $\varepsilon = 0$, Greenhill's solution*

If $\varepsilon = 0$, equation (3.11) can be solved by the method of separation of variables, in which case the solution has the form

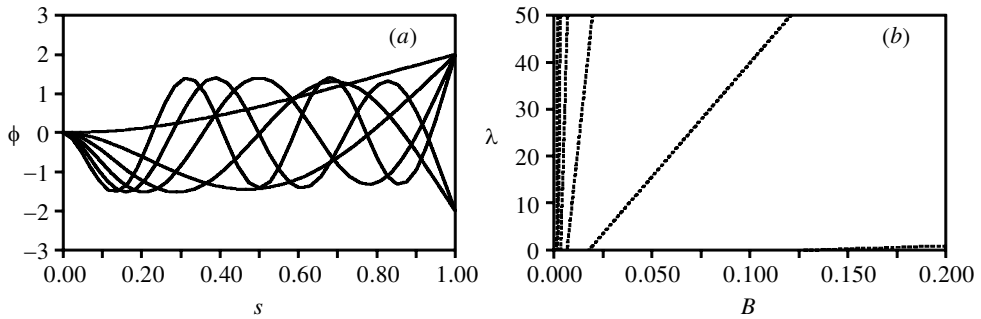
$$u(s, t) = \sum \phi_n(s)(A_n \cos \gamma_n t + B_n \sin \gamma_n t), \quad (3.13)$$

where $\phi_n(s)$ are the eigenfunctions of the self-adjoint differential equation

$$M\phi_n - \lambda_n\phi_n \equiv B\phi_n'''' + [(1 - s)\phi_n']' - \lambda_n\phi_n = 0, \quad (3.14)$$

Table 1. The five lowest eigenvalues of equation (3.14) as a function of B

B	λ_1	λ_2	λ_3	λ_4	λ_5
0.002 142	-27.944	-27.093	-6.6954	-1.9270	0.000 00
0.003 503	-17.375	-10.602	-1.6489	0.000 00	49.992
0.006 734	-6.2896	-2.155 9	0.000 00	45.567	179.75
0.017 864	-1.5254	0.000 00	42.600	209.12	625.21
0.10	-0.343 15	39.884	355.63	1401.7	3906.5
0.127 594	0.000 00	53.285	460.68	1813.5	5008.7
0.20	0.897 60	88.446	736.32	2871.9	7900.9

Figure 2. (a) Eigenfunctions $\phi(s)$ of (3.14) for $B = 0.2$. (b) Loci of the eigenvalues with B .

with $\lambda_n = \gamma_n^2/\delta$, subject to the boundary conditions (3.12). The summation in equation (3.13) is to be taken over all values of λ_n . The eigenfunctions also satisfy the orthogonality condition

$$\int_0^1 \phi_n(s)\phi_m(s) ds = N_n \delta_{nm}, \quad \text{where } N_n = \int_0^1 \phi_n^2(s) ds \quad (3.15)$$

and δ_{nm} is the Kronecker delta.

The first five eigenvalues $\lambda_n = \gamma_n^2/\delta$ ($= \gamma_n^2 \omega_0^2 \ell/g$ in terms of dimensional quantities) are tabulated against the bending stiffness parameter B in table 1. Also, figure 2 depicts the shapes of the eigenfunctions and the locus of the eigenvalues against B for the first six. Note that each eigenvalue locus appears to vary linearly with B and to pass through zero for some positive B -value. As will be shown shortly, these B -values are given precisely by the zeros of the Bessel function $J_{-1/3}(\frac{2}{3}B^{-1/2})$, the first five of which are $B = 0.127\,594$, $0.017\,864$, $0.006\,734$, $0.003\,503$, $0.002\,142$.

Negative eigenvalues indicate that the deflection of such a column when it is given a small displacement from the upright position will increase without bound. If the eigenvalues are positive then a small displacement from the vertical position will result in bounded lateral oscillations of the column. The conclusion is that if $B > B_{\text{cr}} \approx 0.127\,59$ then $\lambda_i > 0$ for all i . Hence for $B > B_{\text{cr}}$ the upright column is stable. As the bending stiffness B is decreased below this value the column can no longer support its own weight.

In dimensionless terms the column has unit length. When put back in terms of dimensional quantities, the value $B_{\text{cr}} = 0.127\,59$ can be shown as follows to correspond to the value obtained by Greenhill (1881) for ‘the greatest height consistent

with stability that a vertical pole or mast can be made' (see also Timoshenko & Gere 1961, p. 101).

Consider the time-independent problem with u a function of s only. Then equation (3.14) with $\lambda = 0$ becomes

$$Mu = Bu'''' + [(1-s)u']' = 0.$$

This can be integrated once to give

$$Bu''' + (1-s)u' = 0, \quad (3.16)$$

where the constant of integration is zero by the boundary condition $u'''(1) = 0$. This equation is second order in the variable $u'(s)$, and the general solution is

$$u'(s) = \sqrt{1-s} \{C_1 J_{1/3}[\frac{2}{3}B^{-1/2}(1-s)^{3/2}] + C_2 J_{-1/3}[\frac{2}{3}B^{-1/2}(1-s)^{3/2}]\}, \quad (3.17)$$

where $J_{\pm 1/3}$ are the Bessel functions of order plus and minus one-third. Application of the boundary condition $u''(1) = 0$ results in $C_1 = 0$, and, finally, application of the boundary condition $u'(0) = 0$ gives

$$u'(0) = C_2 J_{-1/3}(\frac{2}{3}B^{-1/2}) = 0. \quad (3.18)$$

Thus $(\frac{2}{3}B_{\text{cr}}^{-1/2}) \approx 1.86635$, which is the lowest zero of this Bessel function. The other zeros of this Bessel function give the zeros of the other eigenvalue loci plotted in figure 2*b*. In terms of dimensional quantities this means that the condition for stability of a column against buckling under its own weight is that its length must be less than

$$\ell_{\text{cr}} = 1.98365(B/mg)^{1/3}. \quad (3.19)$$

4. Asymptotic analysis of the linear stability equation

A two-timing asymptotic analysis of equation (3.11) for $|\varepsilon| \ll 1$ is now described in order to understand how the linear stability condition $B > B_{\text{cr}}$ deforms under small forcing. An expansion is made in the neighbourhood of the point $\varepsilon = 0$, $B = B_{\text{cr}} \approx 0.12759$, with δ free, in order to establish how the linear stability curve emanating from $B = B_{\text{cr}}$ in the (B, ε) parameter plane depends on δ . Thus, a slow time-scale $\tau = \varepsilon t$ is now introduced, and B and u are expanded in powers of ε as follows (cf. Kevorkian & Cole (1981, p. 152)):

$$\left. \begin{aligned} B &= B_0 + \varepsilon B_1 + \varepsilon^2 B_2 + \cdots \quad (B_0 = B_{\text{cr}}) \\ u(s, t; \varepsilon) &= u_0(s, t, \tau) + \varepsilon u_1(s, t, \tau) + \varepsilon^2 u_2(s, t, \tau) + \cdots \end{aligned} \right\} \quad (4.1)$$

Substitution of these expansions into (3.11) leads to the following set of equations for u_0, u_1 and u_2 :

$$\frac{\partial^2 u_0}{\partial t^2} + \delta L(u_0) + \delta B_0 u_0'''' = 0, \quad (4.2)$$

$$\frac{\partial^2 u_1}{\partial t^2} + \delta L(u_1) + \delta B_0 u_1'''' = \cos t L(u_0) - \delta B_1 u_0'''' - 2 \frac{\partial^2 u_0}{\partial \tau \partial t}, \quad (4.3)$$

$$\frac{\partial^2 u_2}{\partial t^2} + \delta L(u_2) + \delta B_0 u_2'''' = \cos t L(u_1) - \delta B_1 u_1'''' - \delta B_2 u_0'''' - 2 \frac{\partial^2 u_1}{\partial \tau \partial t} - \frac{\partial^2 u_0}{\partial \tau^2}, \quad (4.4)$$

where

$$L(u) = [(1-s)u']'.$$

Boundary conditions (3.12) are applied to each of u_0, u_1 and u_2 , and solutions are sought that are bounded as both t and τ become large.

Notice that equation (4.2) is just (3.11) with $\varepsilon = 0$ whose general solution at $B_0 = B_{\text{cr}}$ is a linear sum of sinusoids times eigenfunctions given in (3.13). Since the aim is to find the behaviour of the solution in the neighbourhood of the linear stability boundary, the particular solution to (4.1) that should be taken is the neutrally stable mode of the static problem. That is, choose $u_0 = f_0(\tau)\phi_1(s)$, where ϕ_1 is given by the integral of (3.17) with $C_1 = 0$ and $B = B_{\text{cr}}$. Hence u_0 is independent of t , but may depend on the slow time τ .

When this result is substituted into (4.3) it becomes

$$\frac{\partial^2 u_1}{\partial t^2} + \delta L(u_1) + \delta B_0 u_1'''' = \cos t f_0(\tau) L(\phi_1) - \delta B_1 f_0(\tau) \phi_1''''(s),$$

which has a particular solution

$$u_1 = [F_0(s) + \cos t F_1(s)] f_0(\tau), \quad (4.5)$$

where F_0 and F_1 satisfy the equations

$$B_0 F_0'''' + L(F_0) = B_1 \phi_1'''' , \quad (4.6)$$

$$\delta B_0 F_1'''' + \delta L(F_1) - F_1 = L(\phi_1). \quad (4.7)$$

Now the homogeneous part of (4.6) has non-trivial solution proportional to ϕ_1 and so the inhomogeneous equation has a bounded solution only if the right-hand side is orthogonal to u_0 . Therefore $B_1 = 0$, and F_0 is proportional to ϕ_1 , and thus $F_0(s)$ can be absorbed into a rescaling of the $O(1)$ part of the solution u_0 , so that without loss of generality F_0 can be set to zero, which leaves

$$u_1 = F_1(s) f_0(\tau) \cos t. \quad (4.8)$$

Finally, when solutions u_0 and u_1 are substituted into the right-hand side of equation (4.4) it becomes

$$\begin{aligned} \frac{\partial^2 u_2}{\partial t^2} + \delta B_0 u_2'''' + \delta L(u_2) &= \frac{1}{2}(1 + \cos 2t) f_0(\tau) L(F_1)(s) \\ &\quad - 2 \sin t \frac{df_0}{d\tau} F_1(s) - \frac{d^2 f_0}{d\tau^2} \phi_1(s) - \delta B_2 f_0(\tau) \phi_1''''(s). \end{aligned} \quad (4.9)$$

The particular integral of this equation is

$$u_2 = G_0(s, \tau) + \cos 2t G_1(s, \tau) + \sin t G_2(s, \tau),$$

where

$$\begin{aligned} \delta[B_0 G_0'''' + L(G_0)] &= [\tfrac{1}{2}L(F_1) - \delta B_2 \phi_1'''] f_0(\tau) - \frac{d^2 f_0}{d\tau^2} \phi_1(s), \\ \delta[B_0 G_1'''' + L(G_1)] - 4G_1 &= \tfrac{1}{2} f_0(\tau) L(F_1), \\ \delta[B_0 G_2'''' + L(G_2)] - G_2 &= 2 \frac{df_0}{d\tau}. \end{aligned} \quad (4.10)$$

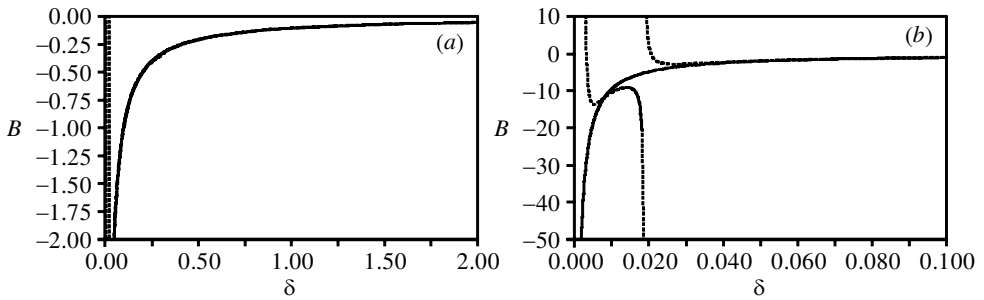


Figure 3. (a) The locus of B_2 against δ defined by the more restrictive condition (4.14) (solid line) and by the more general integral condition (4.16) (solid and dashed lines). (b) Shows a blow-up of (a) for small δ .

Again a necessary condition for (4.10) to have a solution is that its right-hand side be orthogonal to $\phi_1(s)$, the non-trivial solution to the homogeneous part. This condition leads to the following equation for the slow-time-dependent amplitude function $f_0(\tau)$:

$$\frac{d^2 f_0}{d\tau^2} - \alpha^2 f_0 = 0, \quad (4.11)$$

where

$$\alpha^2 = \frac{\int_0^1 \left\{ \frac{1}{2} L(F_1) - \delta B_2 \phi_1''''(s) \right\} \phi_1(s) ds}{\int_0^1 [\phi_1(s)]^2 ds}, \quad (4.12)$$

where F_1 solves (4.7).

The condition for the function $f_0(\tau)$ to be bounded is $\alpha^2 < 0$. If $\alpha^2 > 0$ the solution is unbounded on the slow time-scale, and the stability boundary is determined by the condition that the numerator in equation (4.12) is equal to zero.

In seeking zeros of the integral (4.12) we note that a class of solutions can be found for which the integrand is identically zero. That is

$$\frac{1}{2} L(F_1) - \delta B_2 \phi_1'''' = 0. \quad (4.13)$$

Substitution of this relation into (4.7), and use of equation (3.14) with $n = 1$, $B = B_{\text{cr}}$ so that $\lambda_1 = 0$ leads to a single equation for F_1 ,

$$\delta B_0 F_1'''' + \left(\delta + \frac{B_0}{2\delta B_2} \right) L(F_1) = F_1, \quad (4.14)$$

subject to the usual boundary conditions (3.12). We then seek values B_2 that lead to a non-trivial solution of (4.14). A numerically obtained solution locus $B_2(\delta)$ is presented as the solid line in figure 3.

Note that B_2 is negative for all $\delta > 0$, asserting that the Indian rope trick is possible, that is the stability boundary occurs for $B < B_{\text{cr}}$. Note also that $B_2(\delta)$ is approximately $-0.1/\delta$ over a large range of δ . More specifically the numerical data suggest

$$B_2 = -C(\delta)/\delta \quad \text{for some function } C \quad (4.15)$$

where

$$C(\delta) \rightarrow \begin{cases} 0.102, & \text{as } \delta \rightarrow \infty, \\ 0.0922, & \text{as } \delta \rightarrow 0. \end{cases}$$

For example, $B_2(10.0) = -0.010\,15$, $B_2(1) = -0.100\,79$, $B_2(0.1) = -0.990\,73$ and $B_2(0.0001) = -926.28$.

Now let us return to the orthogonality (non-resonance) condition (4.12). Recall that equation (4.14) was only a sufficient condition for a solution. After integration by parts, a zero of (4.12) can be reformulated to directly define B_2 as

$$B_2 = \frac{\frac{1}{2} \int_0^1 L(F_1) \phi_1 \, ds}{\delta \int_0^1 (\phi_1'')^2 \, ds}, \quad (4.16)$$

which can be evaluated numerically once (4.7) is solved for F_1 . Solutions to this problem were found to contain the solution $B_2(\delta)$ to (4.14) but also to admit additional solution branches. Three of these solution branches are displayed as dashed lines in figure 3, where they appear to bifurcate from the solid line $B_2(\delta)$. We shall return to a discussion of what these additional branches mean at the end of the next section. For the meantime let us restrict attention to those values of δ (sufficiently large) for which the linear stability boundary appears to be given by a unique curve.

Consider the physical interpretation of the result (4.15). We know that the rod is statically stable for $B > B_{\text{cr}}$. Upon reintroduction of dimensional variables, the condition for the dynamic problem to be stable is now

$$\left(\frac{B}{mg\ell^3} \right) = \bar{B} > B_{\text{cr}} - \frac{C\varepsilon^2}{\delta} = B_{\text{cr}} - C \left(\frac{\Delta}{\ell} \right)^2 \left(\frac{\omega_0^2 \ell}{g} \right), \quad (4.17)$$

where Δ is the dimensional amplitude of the support vibration. Now, using (3.19), the definition of ℓ_{cr} , the critical length at which the static rod can just support itself, is

$$\ell_{\text{cr}} = B_{\text{cr}}^{-1/3} \left(\frac{B}{mg} \right)^{1/3},$$

and hence (4.17) can be rearranged to read

$$\omega_0^2 \Delta^2 > \frac{B_{\text{cr}} \ell g}{C} \left(1 - \frac{\ell_{\text{cr}}^3}{\ell^3} \right) \approx (1.27 \dots) \ell g \left(1 - \frac{\ell_{\text{cr}}^3}{\ell^3} \right). \quad (4.18)$$

This formula gives the left-hand stability boundary in the frequency–amplitude domain. It remains to be seen whether this asymptotics is valid, and whether there is also a right-hand stability boundary. In an attempt to answer both questions, we now turn to numerics.

5. Numerical linear stability analysis

Equation (3.11) will be considered numerically for $\varepsilon \neq 0$. A harmonic balance approach will be used to compute linear stability boundaries, by analogy with the

method that is applied to the Mathieu equation (see, for example, Jordan & Smith 1986, §9.3). For the Mathieu equation, which is an ODE, stability boundaries are thus given by solutions of coupled algebraic equations. For the present case, where the underlying equation is a PDE, this will lead to sets of coupled boundary-value problem (BVP) ODEs. These infinite sets will first be truncated to a finite collection and then solved using a standard BVP-solver, specifically the software AUTO (Doedel *et al.* 1997).

(a) *Floquet theory*

By analogy with the Mathieu equation, stability regions in a parameter plane are bounded by curves which correspond to Floquet multipliers $+1$ or -1 . Consider first solutions to (3.11) corresponding to multipliers $+1$. Such solutions are pure periodic with period 2π and may be written as

$$u(s, t) = a_0(s) + \sum_{n=1}^{\infty} (a_n(s) \cos nt + b_n(s) \sin nt), \quad (5.1)$$

where the a_n satisfy the differential equations

$$\left. \begin{aligned} \delta(Ba_0'''' + L(a_0)) &= \frac{1}{2}\varepsilon L(a_1), \\ \delta(Ba_1'''' + L(a_1)) &= a_1 + \varepsilon L(a_0) + \frac{1}{2}\varepsilon L(a_2), \\ \delta(Ba_n'''' + L(a_n)) &= n^2 a_n + \frac{1}{2}\varepsilon L(a_{n-1}) + \frac{1}{2}\varepsilon L(a_{n+1}), \quad n = 2, 3, \dots \end{aligned} \right\} \quad (5.2)$$

Here $L(u) = [(1-s)u']'$. Similarly, the b_n satisfy

$$\left. \begin{aligned} \delta(Bb_1'''' + L(b_1)) &= b_1 + \frac{1}{2}\varepsilon L(b_2), \\ \delta(Ba_n'''' + L(b_n)) &= n^2 b_n + \frac{1}{2}\varepsilon L(b_{n-1}) + \frac{1}{2}\varepsilon L(b_{n+1}), \quad n = 2, 3, \dots \end{aligned} \right\} \quad (5.3)$$

All $a_n(s)$ and $b_n(s)$ are subject to the boundary conditions (3.12). Note that the system for the cosine modes is completely decoupled from that for the sine modes.

Floquet multipliers -1 correspond to the existence of periodic orbits of (3.11) with minimal period 4π that also satisfy $u(s, 2\pi + t) = -u(s, t)$. Such modes can be expressed as Fourier series

$$u(s, t) = \sum_{n=0}^{\infty} (a_m(s) \cos mt + b_m(s) \sin mt), \quad \text{for } m = \frac{1}{2}(2n+1), \quad (5.4)$$

where the a_m and b_m satisfy

$$\left. \begin{aligned} \delta(Ba_{1/2}'''' + L(a_{1/2})) &= \frac{1}{4}a_{1/2} + \frac{1}{2}\varepsilon L(a_{1/2}) + \frac{1}{2}\varepsilon L(a_{3/2}) \\ \delta(Ba_m'''' + L(a_m)) &= m^2 a_m + \frac{1}{2}\varepsilon L(a_{m-1}) + \frac{1}{2}\varepsilon L(a_{m+1}), \\ &m = \frac{1}{2}(2n+1), \quad n = 1, 2, \dots, \end{aligned} \right\} \quad (5.5)$$

$$\left. \begin{aligned} \delta(Bb_{1/2}'''' + L(b_{1/2})) &= \frac{1}{4}b_{1/2} - \frac{1}{2}\varepsilon L(b_{1/2}) + \frac{1}{2}\varepsilon L(b_{3/2}) \\ \delta(Bb_m'''' + L(b_m)) &= m^2 b_m + \frac{1}{2}\varepsilon L(b_{m-1}) + \frac{1}{2}\varepsilon L(b_{m+1}), \\ &m = \frac{1}{2}(2n+1), \quad n = 1, 2, \dots, \end{aligned} \right\} \quad (5.6)$$

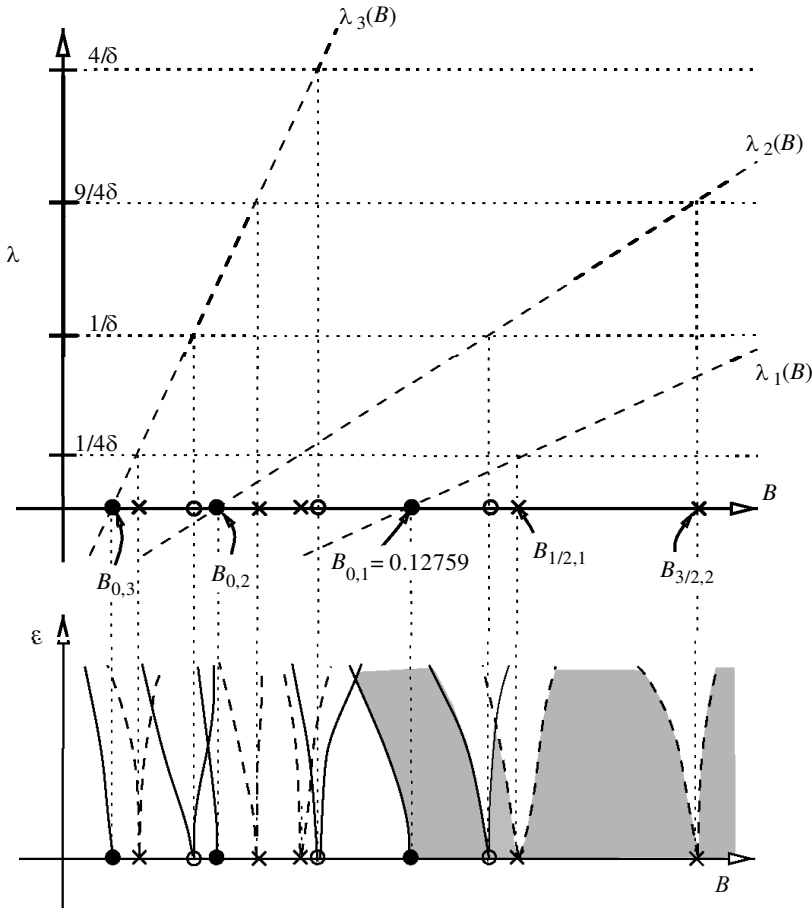


Figure 4. Illustrating the construction of stability boundaries and resonance tongues. The shaded region corresponds to where the vertical solution is stable; solid lines represent transition curves corresponding to Floquet multipliers $+1$ and dashed lines correspond to multipliers -1 .

subject again to the boundary conditions (3.12). Note, as before, that the cosine and sine modes are decoupled.

Non-trivial solutions to (5.2), (5.3), (5.5) or (5.6) correspond to neutral stability surfaces in (B, δ, ε) -space. Now, we can understand some of the properties of these neutral stability surfaces by looking at their bifurcation from the limit $\varepsilon = 0$. Look first at those corresponding to Floquet multipliers $+1$. Non-trivial solutions of (5.2) for $\varepsilon = 0$ are pure in a_n for some n . Such solutions may only be obtained if $B = B_{n,i}(\delta)$, where $B_{n,i}$, for $n = 0, 1, 2, \dots$ and $i = 1, 2, \dots$, are defined by

$$\lambda_i(B_{n,i}) = n^2/\delta, \quad (5.7)$$

where $\lambda_i(B) = \gamma_i^2/\delta$ are the eigenvalues of the rescaled static eigenvalue equation (3.14). Similarly, non-trivial sine mode solutions for $\varepsilon = 0$ are pure in b_n and occur for $B = B_{n,i}(\delta)$ defined by (5.7) for $n = 1, 2, \dots$ and $i = 1, 2, \dots$

We seek branches of solutions in the (B, ε) -plane emanating from $\varepsilon = 0$. From standard bifurcation results, given generic hypotheses then there will be one pure

Table 2. *Convergence of the numerical scheme with number of Fourier components N*

(For each N , the table presents the numerically determined B -values for instability modes with $\varepsilon = 0.05$, $\delta = 0.1$. Data are given for all modes found for $N \leq 5$ which bifurcate from $\varepsilon = 0$ at $B = B_{m,i}$ with $0.035 < B < 0.25$.)

mode (m, i)	B -values				
	$N = 1$	$N = 2$	$N = 3$	$N = 4$	$N = 5$
$\cos(3, 2)$	—	—	0.203 395	0.203 256	0.203 258
$\sin(3, 2)$	—	—	0.203 394	0.203 258	0.203 258
$\sin(\frac{3}{2}, 2)$	—	0.146 726	0.146 567	0.146 567	0.146 567
$\cos(\frac{3}{2}, 2)$	—	0.146 711	0.146 552	0.146 552	0.146 552
$\cos(0, 1)$	0.126 378	0.125 166	0.125 166	0.125 166	0.125 166
$\cos(2, 2)$	—	0.100 564	0.100 374	0.100 374	0.100 374
$\sin(2, 2)$	—	0.100 562	0.100 372	0.100 372	0.100 372
$\sin(\frac{9}{2}, 4)$	—	—	—	—	0.086 151
$\cos(\frac{9}{2}, 4)$	—	—	—	—	0.086 151
$\cos(5, 3)$	—	—	—	—	0.072 375
$\sin(5, 3)$	—	—	—	—	0.072 375
$\sin(\frac{7}{2}, 4)$	—	—	—	0.059 917	0.059 817
$\cos(\frac{7}{2}, 4)$	—	—	—	0.059 918	0.059 817
$\sin(4, 3)$	—	—	—	0.048 780	0.048 668
$\cos(4, 3)$	—	—	—	0.048 780	0.048 668
$\cos(1, 2)$	0.039 411	0.039 935	0.039 934	0.039 935	0.039 935
$\sin(\frac{5}{2}, 3)$	—	—	0.038 965	0.038 839	0.038 839
$\cos(\frac{5}{2}, 3)$	—	—	0.038 965	0.038 839	0.038 839
$\sin(1, 2)$	0.038 517	0.038 202	0.038 200	0.038 201	0.038 201

cosine solution (i.e. with $b_n = 0$ for all n) emanating from $B_{0,i}$ for each i , and two solutions (one pure sines, one pure cosines) emanating from each $B_{n,i}$ for $n \neq 0$. The possibility of mixed sine and cosine solutions would only arise at degenerate points in the (B, ε) -plane where the two uncoupled systems (5.2) and (5.3) simultaneously have non-trivial solutions.

Consider now curves corresponding to Floquet multipliers -1 . Using the same reasoning and notation, these will bifurcate from $\varepsilon = 0$ at $B = B_{m,i}(\delta)$ where $m = \frac{1}{2}(2n+1)$, $n = 0, 1, 2, \dots$, $i = 1, 2, \dots$. Moreover at each bifurcation point there will be two solutions emanating into $\varepsilon > 0$, one a sine mode and one a cosine.

The situation is illustrated qualitatively in figure 4.

(b) Numerical results

The infinite set of linear boundary value problems (5.2), (5.3), (5.5) or (5.6) can be solved numerically by first truncating at $n = N$ for some finite N and solving the finite set using an ODE solver. All results shown are for $N = 4$, that is a coupled system of five fourth-order BVPs for the cosine modes corresponding to Floquet multipliers $+1$ and four BVPs for all other kinds of solution. Note that for $\varepsilon < 0.25$ excellent convergence was found upon increase of N . This convergence is illustrated in table 2 for $\varepsilon = 0.05$, $\delta = 0.1$.

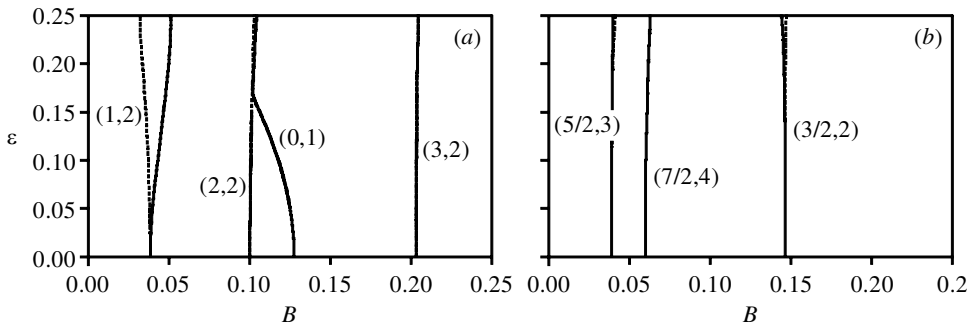


Figure 5. Neutral stability curves in the (B, ε) -plane for $\delta = 0.1$ and $0.035 < B < 0.25$ for (a) Floquet multipliers $+1$ and (b) to multipliers -1 . Solid lines correspond to cosine modes (in phase with the drive) and dashed lines to sine modes (out of phase). Numbers attached to curves correspond to the fundamental angular frequency of the mode as $\varepsilon \rightarrow 0$. Note that, apart from $(0, 1)$, each label corresponds to a pair of curves (one dashed and one solid); where this is not apparent is because the two curves are overlaid on the scale depicted.

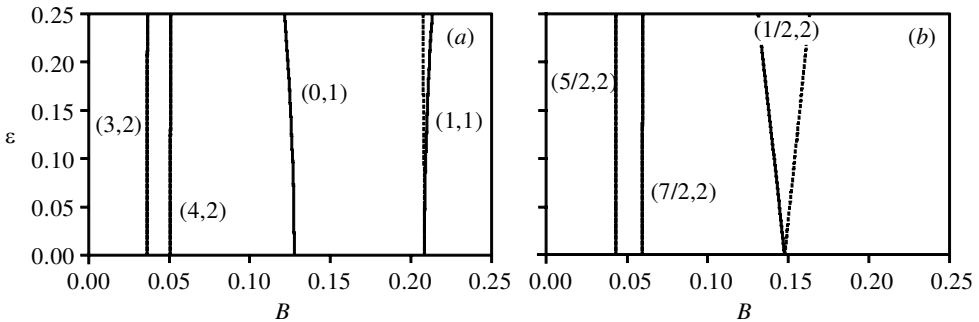


Figure 6. Similar to figure 5 but for $\delta = 1$.

The results for fixed $\delta = 0.1$ are plotted in figure 5, and for $\delta = 1$ in figure 6. Note that the mode that bifurcates from $B_{\text{cr}} = B_{0,1} = 0.127\,594$ bends back to the left. This again suggests that the Indian rope trick is possible. That is, by choosing a $\varepsilon > 0$, there is a region of stability of the rod for $B < B_{\text{cr}}$. There is one caveat to this observation and that is the presence of the infinitely many other resonance tongues. However, we have computed all other such tongues that occur for $0.035 < B < 0.25$ which have $n < 4$ (i.e. have frequency greater than 4 in the limit $\varepsilon \rightarrow 0$). Note that even the tongues with $n = 2$ are remarkably thin. We conjecture that there is still an open region of stability even though there are infinitely many incursions of resonance tongues for higher n (see § 6 for further discussion on this point).

(c) Comparison between asymptotics and numerics

Figure 7 shows the curve $B(\varepsilon)$ for the $(0, 1)$ mode computed in the previous section compared with what the asymptotic result (4.15) gives using the numerically determined value of B_2 . Note how for small ε the two curves are almost overlaid showing the excellent agreement between the asymptotics and numerics.

We are also now in a position to suggest an explanation of the extra (dashed) curves appearing in figure 3 for small δ . By definition of F_1 the bifurcation points of these

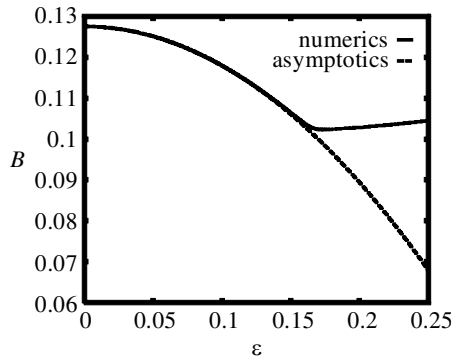


Figure 7. Comparison between theory and asymptotics for the neutral stability curve bifurcating from B_{cr} for $\delta = 0.1$.

new curves from the main solid line correspond to when the component of $\cos t$ in the solution undergoes a non-trivial multiplicity. Looking at figure 4, these points occur when for a given value of delta the value $B_0 = B_{0,1} = 0.12759\dots$ is the root point of more than one tongue. One would correspond to the $(0, 1)$ ‘primary’ instability and the other to some $(1, n)$ tongue for some n . The extra curves bifurcating from these points in the (B, δ) -plane then pick up not the ε^2 component of the primary instability curve, but the ε^2 component of the higher-order tongue. It is then not surprising that these extra curves should extend towards $|B| \rightarrow \infty$ as delta varies, since the value B_0 is no longer the root point of these tongues. There is also likely to be extra complexity due to ‘mode interaction’ at these codimension-two degenerate points. The overall conclusion is that only the solid line in figure 3 is relevant for the asymptotic expression of the ‘primary’ $(0, 1)$ resonance tongue. However, near these extra codimension-two points where tongues collide the region of upside-down stability may in fact vanish for small ε .

6. Conclusion

As far as we are aware, this is the first direct study via a continuum model of what has been referred to (Acheson 1997, p. 178) as ‘not quite the Indian rope trick’. It is intended to be part of a series of papers that will additionally undertake a nonlinear analysis of the continuum model and perform numerical simulations of the full equations. Although the scope of the present work has been limited to model derivation and linearized analysis, the results are nevertheless appealing.

The main result is the formula (4.18), which predicts a lower bound on the frequency and amplitude of excitation in order for an unstable column to be stabilized by harmonic excitation. The formula is expressed solely in terms of experimentally amenable quantities such as the critical length of the unforced rod. Moreover, in some simple phenomenological experiments performed by Tom Mullin to be presented elsewhere, the broad shape of (4.18) was found by varying ℓ_0 and ω for fixed ε . At present there is some quantitative uncertainty in the experiments (due it would seem in part to the many additional resonances found in the theory) but even given this, we have been unable to find close quantitative agreement yet. More careful experimental comparison is intended to form the subject of future work.

The formula (4.18) does have two further things in its favour. First, we have found good agreement (embodied in figure 7) between this asymptotic result and the numerical Floquet theory. This suggests that the asymptotics gives the correct description of the primary instability threshold *for this model*. (There of course remains the question of whether the modelling assumptions we have made are valid for the bendy curtain wire used in Mullin's experiment.) Second, the functional form of this result—that ω varies inversely with Δ —is reminiscent of Stephenson's lower bound for the inverted pendulum and Acheson's and Otterbein's for N inverted pendula. The issue of quantitative agreement between these formulae upon taking the limit $l_{\text{cr}} \rightarrow \infty$ will be taken up in subsequent work.

While the lower bound on drive frequency and amplitude is qualitatively consistent with the coupled rigid pendulum analogy, the issue of an upper stability bound on drive frequency or amplitude is much more subtle for the continuously flexible problem. Figure 4 explains why. Looking at the (B, ε) -plane for fixed δ , there are infinitely many resonance tongues emanating from $\varepsilon = 0$. Each tongue may be labelled by a pair of integers (m, i) with m corresponding to the harmonic component in the response and i corresponding to the spatial mode number. Therefore, by choosing appropriately the way in which m and i tend to infinity, any finite interval of the positive B -axis will be the root point of infinitely many tongues. The ordering of these tongues is highly dependent on δ . This feature contrasts with the situation for N rigid pendulums viewed in the equivalent of the (ε, δ) parameter-plane. There, only finitely many resonance tongues emanate from a finite portion of the δ -axis and hence it is possible to say which is the nearest instability boundary to the fundamental boundary. This leads to a neat upper bound on the forcing frequency and amplitude in that case (Acheson 1993), which is not possible here.

In fact, with the presence of infinitely many resonance tongues the reader might wonder whether there is likely to be any set of parameter values at which the upside-down position may actually be stable for $B < B_{\text{cr}}$. Put another way, do the infinitely many white incursions into the shaded region of figure 4 fill space? Appealing to the theory of Arnold tongues (see, for example, Broer & Vegter 1992) we can assert that there remains a stability region of positive measure. This is due to the fact that the resonance tongue corresponding to the i th harmonic has local approximation $B = B_n + O(\varepsilon^i)$. This is borne out by the numerics in figures 5 and 6, where even the resonance tongues for $m = 3$ are so thin that their width is undetectable on the scale presented.

Finally, we should comment that the full nonlinear dynamics of this model are likely to be extremely complex. Dynamically, even finite degree of freedom problems of this nature, such as the inverted pendulum (see, for example, Acheson 1995; Broer *et al.* 1998), are known to have a rich structure involving chaotic dynamics and curious 'multiple nodding' oscillations. Pure static problems (see, for example, Hunt & Everal 1999) on supercritical elastic buckling have also been shown to exhibit complexity in their response due to the interaction between resonance tongues. Near points at which stability boundaries cross (such as near $\varepsilon = 0.15$, $B = 0.1$ in figure 5a) the continuous model studied here is likely to incorporate elements of both these static and dynamic problems, and maybe much more!

The authors thank David Acheson, Tom Mullin and John Maddocks for sharing their insights into this problem with us. W.B.F. thanks Les Farnell for performing some preliminary numerical

calculations. The research reported in this paper was supported by a grant from the US National Textile Center through Clemson University to W.B.F., and by an Australian Research Council Large Grant. The work of A.R.C. was also supported by the UK EPSRC with whom he holds an Advanced Fellowship.

References

- Acheson, D. 1993 A pendulum theorem. *Proc. R. Soc. Lond. A* **443**, 239–245.
- Acheson, D. 1995 Multiple-nodding oscillations of a driven inverted pendulum. *Proc. R. Soc. Lond. A* **448**, 89–95.
- Acheson, D. 1997 *From calculus to chaos: an introduction to dynamics*. Oxford University Press.
- Acheson, D. & Mullin, T. 1993 Upside-down pendulums. *Nature* **366**, 215–216.
- Antman, S. S. 1995 *Nonlinear problems of elasticity*. Applied Mathematical Sciences 107. Springer.
- Broer, H. & Vegter, G. 1992 Bifurcation aspects of parametric resonance. *Dynam. Rep.* **1**, 1–53.
- Broer, H., Hoveijn, I. & van Noort, M. 1998 A reversible bifurcation analysis of the inverted pendulum. *Physica D* **112**, 50–63.
- Doedel, E., Champneys, A., Fairgrieve, T., Kuznetsov, Y., Sandstede, B. & Wang, X. 1997 AUTO97 continuation and bifurcation software for ordinary differential equations. Available by anonymous ftp from ftp.cs.concordia.ca, directory pub/doedel/auto.
- Fraser, W. & Stump, D. 1998 Yarn twist in the ring-spinning balloon. *Proc. R. Soc. Lond. A* **454**, 707–723.
- Greenhill, A. G. 1881 Determination of the greatest height consistent with stability that a pole or mast can be made, and of the greatest height to which a tree of given proportions can grow. *Proc. Camb. Phil. Soc.* **IV**, 65–73.
- Hunt, G. & Everal, P. 1999 Arnold tongues and mode-jumping in the supercritical post-buckling of an archetypal elastic structure. *Proc. R. Soc. Lond. A* **455**, 125–140.
- Hurst, C. 1996 The Indian rope trick explained. *Aust. Math. Soc. Gazette* **23**, 154–159.
- Jordan, D. W. & Smith, P. 1986 *Nonlinear ordinary differential equations*, 2nd edn. Oxford University Press.
- Kevorkian, J. & Cole, J. 1981 *Perturbation methods in applied mathematics*. Springer.
- Love, A. 1927 *A treatise on the mathematical theory of elasticity*, 4th edn. Cambridge University Press.
- Otterbein, S. 1982 Stabilisierung des n -pendels und der indische seiltrick. *Arch. Ration. Mech. Analysis* **78**, 381–393.
- Stephenson, A. 1908 On a new type of dynamical stability. *Mem. Proc. Manch. Lit. Phil. Soc.* **52**, 1–10.
- Timoshenko, S. & Gere, J. 1961 *Theory of elastic stability*, 2nd edn. New York: McGraw-Hill.